Influence of Modeling Errors in the Boundary Element Analysis of EEG Forward Problems upon the Solution Accuracy

Do-Won Kim[1], Young-Jin Jung[1], Chang-Hwan Im[1,2]

[1]*Department of Biomedical Engineering, Yonsei University, Wonju, Republic of Korea*
[2]*Institute of Medical Engineering, Yonsei University, Wonju, Republic of Korea*
(Received December 18, 2008. Accepted February 16, 2009)

Abstract

Accurate electroencephalography (EEG) forward calculation is of importance for the accurate estimation of neuronal electrical sources. Conventional studies concerning the EEG forward problems have investigated various factors influencing the forward solution accuracy, e.g. tissue conductivity values in head compartments, anisotropic conductivity distribution of a head model, tessellation patterns of boundary element models, the number of elements used for boundary/finite element method (BEM/FEM), and so on. In the present paper, we investigated the influence of modeling errors in the boundary element volume conductor models upon the accuracy of the EEG forward solutions. From our simulation results, we could confirm that accurate construction of boundary element models is one of the key factors in obtaining accurate EEG forward solutions from BEM. Among three boundaries (scalp, outer skull, and inner skull boundary), the solution errors originated from the modeling error in the scalp boundary were most significant. We found that the nonuniform error distribution on the scalp surface is closely related to the electrode configuration and the error distributions on the outer and inner skull boundaries have statistically meaningful similarity to the curvature distributions of the boundary surfaces. Our simulation results also demonstrated that the accumulation of small modeling errors could lead to considerable errors in the EEG source localization. It is expected that our finding can be a useful reference in generating boundary element head models.

Key words : Boundary element method (BEM), electroencephalography(EEG), forward problem, solution accuracy

Ⅰ. INTRODUCTION

Electroencephalography (EEG) and magnetoencephalography (MEG) are noninvasive human brain imaging devices to estimate neural electrical activities in human cerebral cortex using electromagnetic field measurements outside the head. Accurate EEG or MEG forward calculation is one of the important factors to obtain accurate EEG or MEG source estimates [1]. Particularly in EEG, realistic volume conductor models and accurate forward solver are crucial since the volume current conduction is highly affected by the low conductivity value of a skull [2]. Early studies concerning the EEG source localization used approximated volume conductor models such as a single sphere model [3] and a concentric multi-sphere model [4], to solve the neuroelectric forward problems. In those models, the EEG forward problem could be described with simple analytic formula, which made it easy to calculate the forward potential field in relatively short time even without any anatomical information. However, the approximated models do not guarantee accurate inverse solutions especially around some brain regions where the difference between real head geometry and the approximated head geometry is significant [1]. As high performance computer systems were developed and high-resolution medical images could be readily obtained, people became interested in calculating the EEG forward problems more accurately by means of numerical techniques such as boundary element method (BEM) and finite element method (FEM). BEM is a numerical technique used for calculating the surface potential generated by current sources located in a piecewise homogeneous volume conductor. It has been proven that BEM can provide reasonable accuracy in the EEG (or MEG) forward problems

Corresponding Author : Chang-Hwan Im, Ph.D.
Department of Biomedical Engineering, Yonsei University, 234 Maeji-ri, Heungeop-myun, Wonju-si, Kangwon-do, 220-710 Korea
Tel : +82-33-760-2792 / Fax : +82-33-760-2197
E-mail : ich@yonsei.ac.kr.
This work was supported by the Korea Research Foundation Grant funded by the Korean Government (KRF-2008-521-D00586).

[1,2,5]. FEM is also a promising method for the EEG forward problems since it can potentially consider the inhomogeneous and anisotropic volume conductor models [6-9]. Nevertheless, since the inhomogeneous and anisotropic electrical conductivity distribution of a human head cannot be estimated accurately even with the currently best imaging modalities, BEM has been the most widely used approach for the EEG forward calculations.

There are various factors affecting the accuracy of the BEM-based EEG forward solution. Accurate conductivity information is obviously an important factor for the accurate forward solution regardless of the numerical methods [10]. The tessellation patterns of the boundary elements and the number of boundary elements can also affect the forward solution accuracy [11]. More importantly, the extraction of accurate realistic boundaries is required to obtain accurate forward solutions from BEM [12].

The boundary element model of a subject has been usually obtained by the segmentation of the subject's magnetic resonance imaging (MRI) or computed tomography (CT) images [13]. Although various algorithms have been introduced to create the boundary element models from the medical images automatically [14-16], user intervention is still needed especially when the head MRI data are spatially inhomogeneous or have low contrast [17]. Moreover, manual segmentation is required when only head CT images are available, because CT usually does not provide sufficient contrast between the different head tissues. For cases when anatomical images are not available, approximated boundary element models including skin, skull, and brain can be derived from the head shape data obtained with a 3-D digitizer [17, 18]. Similarly, Fuchs et al. used a standardized head model with transformed electrode locations [19]. The previous studies demonstrated that the approximated boundary element models could give more accurate solutions than spherical head models, but the modeling errors were still significant when compared to the realistic head models extracted from medical images. As listed above, although various segmentation methods have been introduced to generate boundary element head models, potential modeling errors originated from manual segmentation processes, model approximation, and incomplete automatic segmentation still exist.

To the best of our knowledge, the following issues still need to be investigated: 1) Huiskamp et al. [12] investigated the influence of the segmentation methods to generate the boundary element models on the solution accuracy, but they did not investigate which parts of the boundary element model are comparatively more sensitive to the modeling errors. 2) After the investigation on the sensitivity distribution, the relationship between the sensitivity distribution and several modeling factors needs to be investigated. 3) We still need more references concerning the influence of the modeling errors on the solution accuracy of the BEM-based EEG forward calculation.

In the present study, we investigated the above issues through computer simulations. We first assumed 18 evenly-distributed equivalent current dipole (ECD) locations and slightly deformed a part of the boundary element model segmented from standard head MRI data. We then investigated which boundary or part of the boundary is relatively more sensitive to the small geometrical variation. Finally, we compared the changes of the EEG forward solution originated from the deformation of the boundary element model with those arising from the variation of ECD source locations, in order to estimate the influence of the modeling errors on the EEG source localization.

II. METHODS

A three-layer boundary element model, consisting of inner and outer skull boundaries and scalp surface, were generated using CURRY5 for windows (Compumedics, Inc., El Paso,

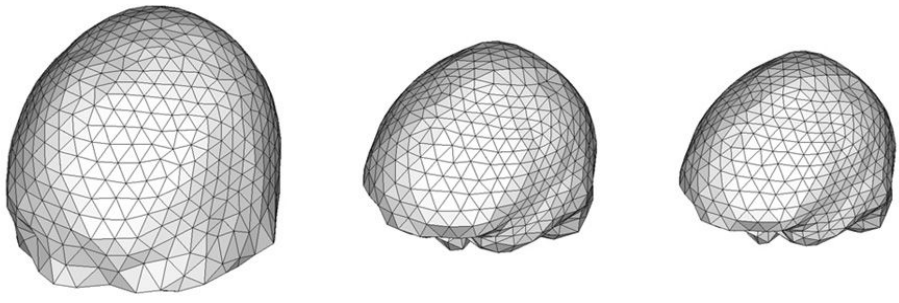

Fig. 1. Boundary element model for the EEG forward calculation (scalp, outer skull, and inner skull boundaries from left to right). 1,779 surface nodes and 3,546 boundary elements were generated. Outer skull boundary was generated by simply scaling the inner skull boundary.

TX) from MNI standard head MRI [20]. The boundary element model consisted of 1,779 surface nodes and 3,546 boundary elements. To quantitatively compare the difference of sensitivity distributions between the inner and outer skull boundaries, the outer skull boundary was generated by simply scaling the inner skull boundary, which is not a crude approximation considering the conventional boundary element models used in literatures (e.g. see [17]). The skull thickness was assumed to be 7 mm and both boundaries had the identical shape and mesh structure. We adopted such an approximation because different geometrical shapes of the boundaries can make it difficult to objectively compare the influences of the modeling errors arising in the inner and outer skull boundaries on the forward solution. Fig. 1 shows the boundary element model used in the present study. The relative conductivity values of the brain, skull, and scalp were assumed to be 1, 1/16, and 1, respectively [10, 21]. We assumed 99 electrodes attached on the scalp surface according to the extended 10-10 electrode system (see Fig. 4 for the electrode configuration). 18 evenly-distributed ECD locations were then determined by placing identical spheres inside the inner skull boundary without overlapping with each other (see Fig. 2). For each of the locations, three unit ECDs with different directional vectors (one radial and two tangential directions) were placed.

For the BEM computations, we have used first-order node-based boundary elements and applied isolated skull approach (ISA), in which the skull is modeled as a perfect insulator and the results of the preliminary field calculations are then mapped back into the multi-shell volume conductor model [2]. The BEM solver was coded with Fortran 90 and all variables were stored as double-precision real numbers for the accurate error estimation. LU decomposition was used for solving the system matrix equation. The BEM solver was executed using an AMD Athlon(tm) 64 X2 Dual Core Processor 4000+ personal computer with 2GByte RAM and the single execution of the program took about 5 minutes.

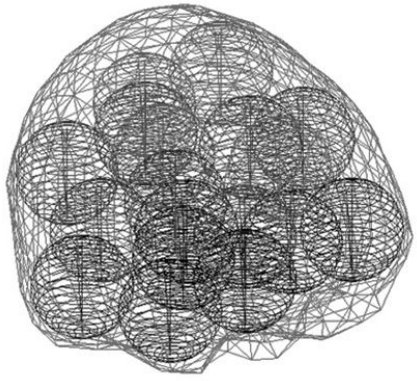

Fig. 2. 18 identical spheres are fitted inside the inner skull boundary of the standard head boundary element model without overlapping with each other. Three orthogonal ECD sources were placed at each center of the sphere.

To investigate the effect of the incorrect boundary element modeling, we first solved the forward problem using the original boundary element model, repeatedly for each ECD. The resultant electric potential values at the 99 electrode locations evaluated for 54 different ECDs were used as a reference data set. To investigate which parts of the boundary element model are relatively more sensitive to the modeling errors, we moved a single boundary node to a new position, which was 1 mm away from its original location in the outward normal direction of the boundary surface, and applied the BEM solver again to the slightly deformed geometry. We then calculated the error between the newly calculated electric potentials and the reference potential data. The error ε_i originated from *i*th boundary node dislocation was calculated using the following equation:

$$\varepsilon_i = \frac{1}{54}\sum_{d=1}^{54}\sqrt{\sum_{k=1}^{99}(\varphi_k - \varphi_{ref,k})^2} \qquad (1)$$

where φ_k is the electric potential of an electrode k evaluated after the *i*th boundary node dislocation, $\varphi_{ref,k}$ is the reference electric potential at the electrode k, k (1 to 99) is the electrode index, and d (1 to 54) is the ECD index.

Evaluating the values of ε_i at all boundary nodes required heavy computational cost since the BEM stiffness matrix was changed by the deformation of the boundary element model and thus matrix inverse processes had to be repeated 1,779 times. It took about a week to evaluate the influence of the modeling error on the solution accuracy.

To investigate the relationship between the error sensitivity distribution of the boundary element model and the curvature distribution of the surfaces, we calculated the local curvature of the tessellated boundary surface model. The curvature of the surface was calculated using a mean curvature algorithm implemented in a freeware called MESHLAB [22].

Ⅲ. RESULTS

After calculating the errors originated from the boundary node dislocation, we first compared the averaged error values in each of the boundaries. The average errors evaluated for the scalp boundary, the outer skull boundary and the inner skull boundary were ε_s = 0.0353 ± 0.0212, ε_{os} = 0.0095 ± 0.0034, and ε_{is} = 0.0105 ± 0.0054, respectively (see Fig. 3). When

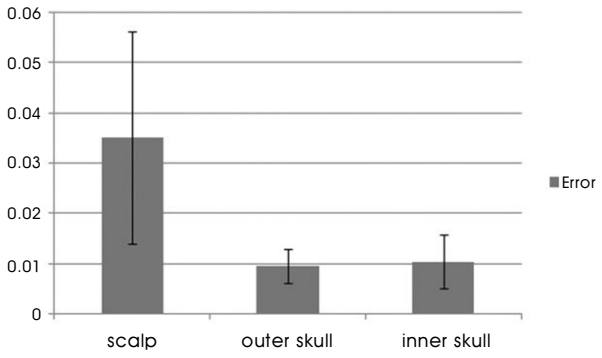

Fig. 3. Averaged forward solution errors originated from 1 mm dislocation of a single boundary element node in scalp, outer skull and inner skull boundaries.

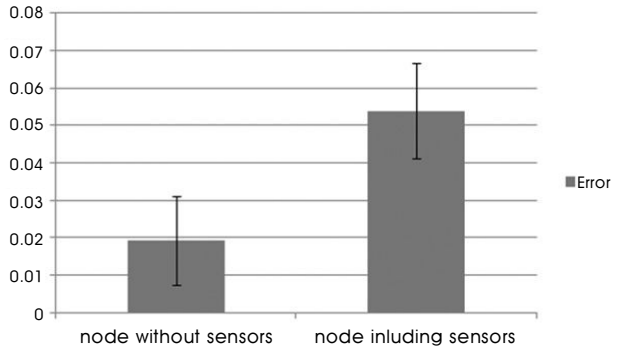

Fig. 5. Comparison of average forward solution errors between nodes in the scalp boundary including electrodes in their neighboring elements and those not including any electrodes.

Wilcoxon ranksum test for equal medians, which is embedded in Matlab statistics toolbox (Mathworks, Inc., Natick, USA), was applied, the errors of the scalp boundary showed significantly meaningful difference from those of the other two boundaries ($p < 0.00001$ in both cases). There was no statistically significant difference between the errors of the outer skull boundary and the inner skull boundary ($p = 0.139$). These results demonstrate that the scalp boundary is more sensitive to the modeling error than the other two boundaries.

Hence, we first focused on the scalp boundary. Fig. 4 shows the normalized error distribution on the scalp surface. Comparing the error distributions with the electrode configuration depicted below, we could observe that nodes close to the electrodes have relatively higher error values. To confirm this visual inspection, we separated the nodes on the scalp boundary into two groups: One group consisted of nodes containing electrodes in its neighboring elements, and the another group consisted of nodes not containing electrodes in its neighboring elements. As depicted in Fig. 5, two groups showed significant difference in their error values (Wilcoxon ranksum test, $p < 0.00001$), which demonstrates that the errors on the scalp boundary are mainly originated from the 'electrode' dislocation. Although the influence of the modeling error in the scalp boundary on the BEM solution accuracy was significant, such a wrong modeling rarely occurs in practical applications. The scalp boundary can be modeled relatively very accurately

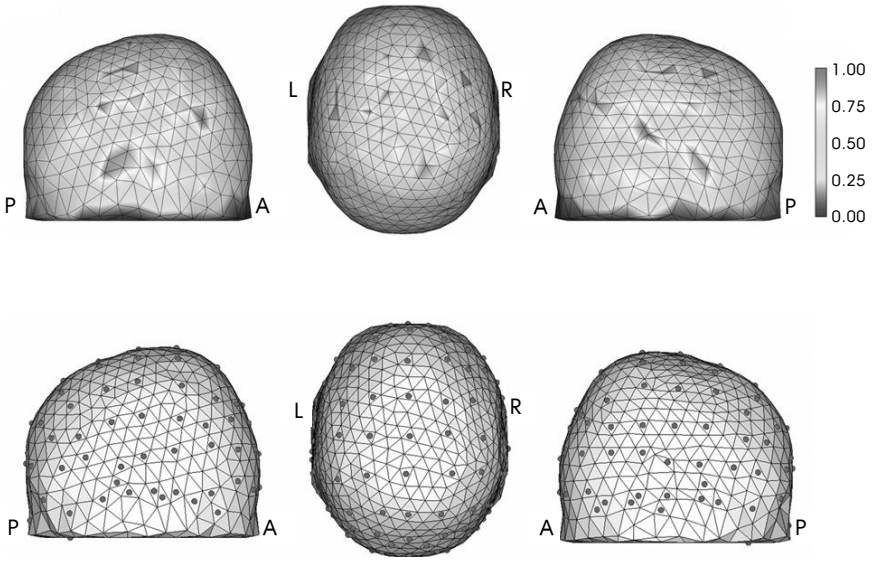

Fig. 4. Normalized error distribution on the scalp surface (upper three figures) and configuration of extended 10-10 electrodes attached on the boundary elements (lower three figures). Three figures show different viewpoints (A: Anterior, P: Posterior). The error values were normalized with respect to the maximum error value.

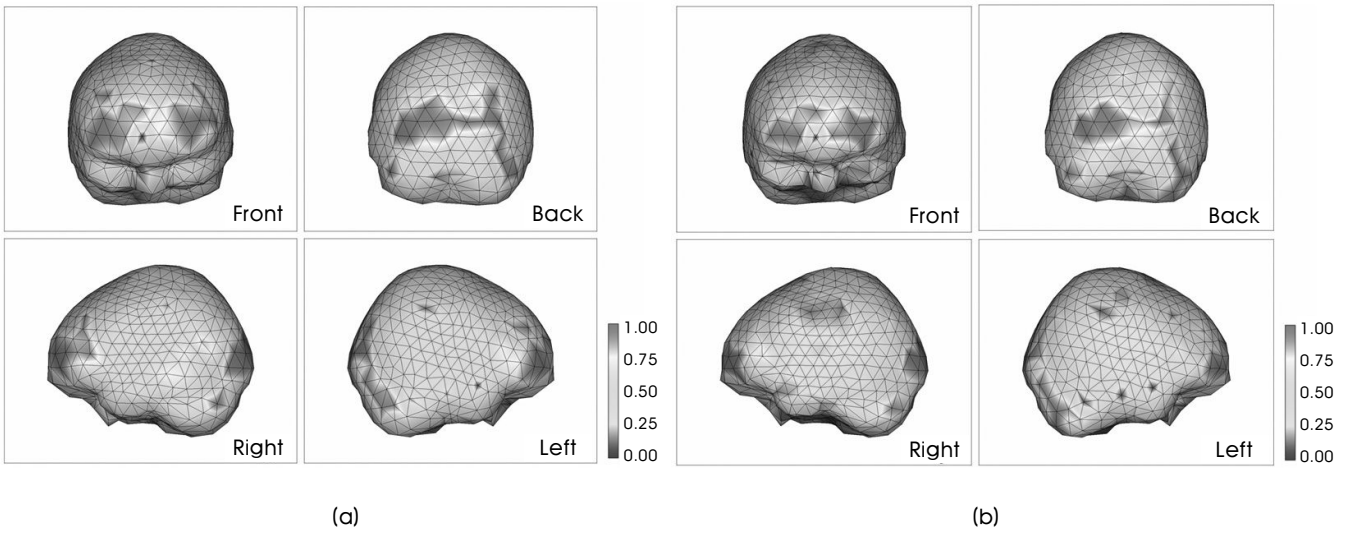

Fig. 6. Forward solution error distribution maps on (a) the outer skull boundary and (b) the inner skull boundary. The values were normalized with respect to the maximum error value.

since the interface between scalp and air is usually very clear in both MRI and CT images. Even when approximated boundary element models are derived from the head shape data obtained with a 3-D digitizer [17, 18] the scalp boundary can also be modeled relatively accurately if accurate head shape data are available. Therefore, the forward solution errors originated from the wrong modeling of the other two boundaries might be more crucial in the practical applications because the outer and inner skull boundaries are often difficult to be modeled accurately, as aforementioned in the introduction section.

Figs. 6a and 6b show the error distribution maps on the outer skull boundary and inner skull boundary, respectively, where the values were normalized with respect to the maximum error value. As expected, both boundaries showed similar error distributions. As seen in both figures, areas close to frontal and occipital lobes showed relatively higher error values than the other areas. After inspecting the distribution carefully, we could make a hypothesis that such an irregular error distribution might be closely related to the curvature of the boundary surface. To test the hypothesis, we calculated the curvature distribution of the inner skull boundary and normalized the curvature values with respect to the maximum value. Fig. 7 shows the normalized curvature distribution,

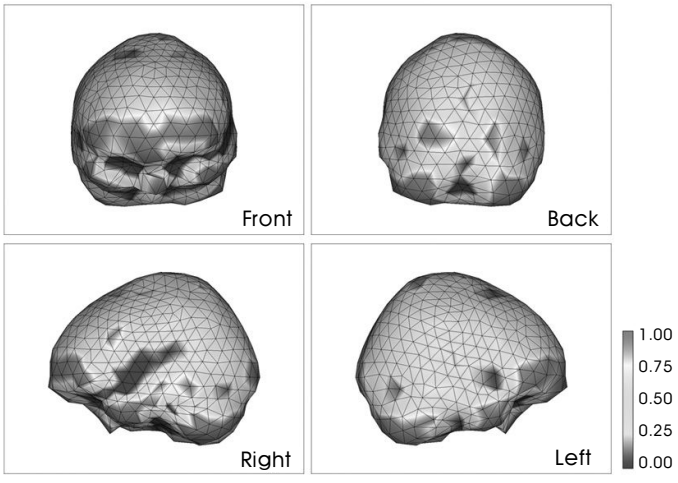

Fig. 7. Normalized curvature distribution in the inner skull boundary. Only inner skull boundary was visualized because the curvature distribution of the outer skull boundary was identical to that of the inner skull boundary.

where only inner skull boundary was visualized because the curvature distribution on the outer skull boundary was identical to that on the inner skull boundary. Comparing Fig. 7 with Fig. 6, we could readily see that the error distribution is similar to the curvature distribution except the regions around inferior Temporal and inferior Occipital lobes. The slight mismatches between the two distributions are thought to be originated from the fact that volume current conduction around the inferior areas does not contribute much to the generation of electric potentials at EEG electrode locations because the electrodes are attached on the scalp, relatively far from the inferior regions.

To confirm the similarity between the two distributions quantitatively, we evaluated correlation coefficient (CC) between them. The CC values calculated for the outer and inner skull boundaries were 0.835 and 0.842, respectively. To test the significance of the CC values, we applied a surrogate test. We first generated 1,000 random values for each boundary node, assuming uniform distribution on [0, 1]. The CC values between the normalized error distribution and the random value distributions were then evaluated for each of the two boundaries. After confirming that the histogram of the two surrogate data sets showed normal distribution, we calculated z-score of the CC values for the outer and inner skull boundaries. The z-scores were 1.874 ($p < 0.05$) for the outer skull boundary and 6.534 ($p < 0.01$) for the inner skull boundary, demonstrating that the error distributions of the outer and inner skull boundaries have statistically significant similarity to the curvature distributions of the surfaces. In other words, the modeling errors in the regions with bigger curvature values have more influence on the forward solution.

To relatively compare the influence of the modeling error with that of another error factor, we slightly shifted the ECD locations toward outward directions. The change of the forward solutions (error norm between the newly calculated potentials and the reference data) was evaluated after moving each ECD to a new location 1 mm away from its original position toward the direction of the normal vector of its nearest boundary node. The average error due to the 1 mm dislocation of the ECD was 0.498 ± 0.134, which is about fifty times larger than the averaged forward calculation error caused by a single boundary node dislocation in the inner skull boundary ($\varepsilon_{is} = 0.0105$). Apparently, the 1 mm displacement of a single boundary node does not affect the forward solution accuracy much, from a practical point of view. However, massive modeling errors occurring in relatively wider areas might result in a significant forward solution error. To confirm this hypothesis, we selected 44 nodes, of which the normalized error values exceeded 0.8, out of the 593 boundary nodes in the inner skull boundary. Most of the selected nodes were distributed in areas with high curvature. We moved the selected nodes simultaneously 1 mm outward and calculated the forward solution error. The forward solution error arising from the simultaneous node dislocation was 0.460, which is comparable to the error due to the 1 mm ECD dislocation. This result demonstrates that modeling errors as low as 1 mm in only 7% area of the whole inner skull boundary can possibly contribute to maximally 1 mm localization error in the ECD source localization. Considering the potential modeling errors reported in literatures ranging from several millimeters to about 1 centimeter [12, 17], the influence of the modeling errors on the solution accuracy should not be underestimated in the practical applications of the EEG source localization.

Ⅳ. DISCUSSIONS AND CONCLUSIONS

In spite of the recent advancements in the computational methodology, the localization of neuroelectric sources from noninvasive EEG recordings still contains considerable uncertainties, which stem from various factors such as lack of accurate conductivity profile of the head, contamination of EEG signals by external noises and artifacts, inaccurate geometrical information, and so on. Hence, people have believed that the EEG source localization results are not accurate enough to be applied directly to some clinical applications such as epilepsy surgery and functional brain mapping for neurosurgery, which usually require very high localization accuracy. Therefore, reducing the uncertainties has been one of the most important issues in the EEG and MEG research society. In the present study, we have investigated the influence of modeling errors on the uncertainty of the EEG forward and inverse solutions.

In the introduction section, we raised some issues which have not been fully investigated in the previous works. We first investigated which parts of the boundary element model are relatively more sensitive to the modeling errors. From the simulation results, we could see that the scalp boundary has the highest sensitivity among the three boundaries and the high sensitivity of the scalp boundary originated mainly from the disposition of the electrode locations. Therefore, good care must be taken in the extraction of the scalp boundary, especially when the scalp boundary is approximated using the head shape data obtained with a 3-D digitizer. Nevertheless, since the scalp boundary can be modeled relatively more accurately than the other boundaries, we focused more on the influence of the modeling errors in the outer and inner skull boundaries on the forward solution accuracy. From the simulation results, relatively higher sensitivity was observed around

Occipital and Frontal lobe areas in both boundaries. By statistically comparing the error distributions on the outer and inner skull boundaries with the curvature distributions of the surfaces, we could confirm that modeling errors in the regions with higher curvature values have more influence on the forward solution accuracy. Another simulation study performed to estimate the influence of the modeling error on the ECD localization accuracy demonstrated that modeling errors as low as 1 mm in areas less than 10% of the whole inner skull boundary can potentially cause about 1 mm localization error in the ECD source localization.

Our results demonstrated again that the accurate volume conductor modeling is of great importance for precise EEG forward calculation. Apart from the scalp boundary that can be modeled relatively accurately, the outer and inner skull boundaries, which often require user intervention or manual process for the segmentation, should be carefully modeled in order to avoid large modeling errors, especially around regions with high curvature. Our findings suggest that the use of approximated boundary element models, of which the modeling errors ranged from several millimeters to about 1 centimeter [17], may not be a wise choice if individual CT or MRI data are available. Although there is no doubt that such approximated models can yield more accurate forward solutions than the spherical volume conductor models, high-quality medical images should be used for clinical applications that require accurate forward solutions. Studies on the new image acquisition/processing approaches to enhancing the image contrast and homogeneity as well as developments of improved segmentation algorithms will help to enhance the accuracy of the EEG forward and inverse solutions.

In any of the numerical techniques used to solve partial differential equations, e.g. BEM, FEM, and finite difference method (FDM), the most straightforward way to enhance the solution accuracy is to increase the number of elements. Particularly in BEM, however, increment of computational costs is considerable when the number of boundary elements is increased, because the BEM computation requires inverse process of a full system matrix. Use of adaptive or graded mesh structures can be one of the solutions to address this issue. It is obvious that generation of more elements around regions with higher sensitivity can reduce the influence of the modeling errors on the forward solution accuracy, because the deformation of the volume conductor model due to the wrong segmentation at some discrete points is reduced thanks to the small element sizes. In the present study, we have shown that the sensitivity of the modeling error to the forward solution is closely related to the curvature distribution of the outer and inner skull boundaries. Therefore, the curvature information might be used as a priori reference to generate graded boundary mesh structures.

In summary, the present study has investigated the influence of modeling errors in the boundary element head models on the accuracy of the EEG forward solutions. We are expecting that our results can be utilized as useful information in generating boundary element head models in practical EEG applications.

REFERENCES

[1] J. C. Mosher, R. M. Leahy, and P. S. Lewis, "EEG and MEG: Forward Solutions for Inverse Methods," *IEEE Trans. Biomed. Eng*., vol. 46, pp. 245-259, 1999.

[2] M. S. Hämäläinen and J. Sarvas, "Realistic conductivity geometry model of the human head for interpretation of neuromagnetic data," *IEEE Trans. Biomed. Eng*., vol. 36, pp. 165-171, 1989.

[3] D. Yao, "Electric potential produced by a dipole in a homogeneous conducting sphere," *IEEE Trans. Biomed. Eng*., vol. 47, pp. 964-966, 2000.

[4] J. C. de Munck, "The potential distribution in a layered anisotropic spheroidal volume conductor," *J. Appl. Phys*., vol. 64, pp. 464-470, 1988.

[5] B, He, T. Musha, Y. Okamoto, S. Homma, Y. Nakajima, and T. Sato, "Electric dipole tracing in the brain by means of the boundary element method and its accuracy," *IEEE Trans. Biomed. Eng*., vol. 34, pp. 406-414, 1987.

[6] C. H. Wolters, A. Anwander, X. Tricoche, D. Weinstein, M. A. Koch, and R. S. MacLeod, Influence of tissue conductivity anisotropy on EEG/MEG field and return current computation in a realistic head model: A simulation and visualization study using high-resolution finite element modeling," *NeuroImage*, vol. 30, pp. 813-826, 2006.

[7] Y. C. Zhang, S. A. Zhu, and B. He, "A Second-Order Finite Element Algorithm for Solving the Three-Dimensional EEG Forward Problem," *Phys. Med. Biol*., vol. 49, pp. 2975-2987, 2004.

[8] Y. C. Zhang, L. Ding, W. van Drongelen, K. Hecox, D. Frim, and B. He, "A Cortical Potential Imaging Study from Simultaneous Extra- and Intra-cranial Electrical Recordings by Means of the Finite Element Method," *NeuroImage*, vol. 31, pp. 1513-1524, 2006.

[9] W. H. Lee, T. S. Kim, M. H. Cho, Y. B. Ahn, and S. Y. Lee, "Methods and evaluations of MRI content-adaptive finite element mesh generation for bioelectromagnetic problems," *Phys. Med. Biol*., vol. 51, pp. 6173-6186, 2006.

[10] J. Haueisen, C. Ramon, M. Eiselt, H. Brauer, and H. Nowak, "Influence of tissue resistivities on neuromagnetic fields and electric potentials studied with a finite element model of the head," *IEEE Trans. Biomed. Eng*., vol. 44, pp. 727-735, 1997.

[11] A. S. Ferguson and G. Stroink, "Factors Affecting the Accuracy of the Boundary Element Method in the Forward Problem - I: Calculating Surface Potentials," *IEEE Trans. Biomed. Eng*., vol. 44, pp. 1139-1155, 1997.

[12] G. Huiskamp, M. Vroeijenstijn, R. van Dijk, G. Wieneke, and A. C. van Huffelen, "The need for correct realistic geometry in the inverse EEG problem," *IEEE Trans. Biomed. Eng*., vol. 46, pp. 1281-1287, 1999.

[13] B. Dogdas, D. W. Shattuck, and R. M. Leahy, "Segmentation of skull in 3-D human MRI using mathematical morphology," *Hum. Brain Mapp*., vol. 26, pp. 273-285, 2005.

[14] M. S. Atkins and B. T. Mackiewich, "Fully Automatic Segmentation of the Brain in MRI," *IEEE Trans. Med. Imag*., vol. 17, pp. 98-107, 1998.

[15] W. M. Wells, W. E. L. Grimson, R. Kikinis, and F. A. Jolesz, "Adaptive segmentation of MRI data," *IEEE Trans. Med. Imag*., vol. 15, pp. 429-442, 1996.

[16] S. J. He, X. Q. Shen, Y. M. Yang, R. J. He, and W. L. Yan, "Research on MRI brain segmentation algorithm with the application in model-based EEG/MEG," *IEEE Trans. Magn*., vol. 37, pp. 3741-3744, 2001.

[17] D. van 't Ent, J. C. de Munck, and A. Kaas, "A Fast Method to Derive Realistic BEM Models for E/MEG Source Reconstruction," *IEEE Trans. Biomed. Eng*., vol. 48, pp. 1434-1443, 2001.

[18] J. Koikkalainen and J. Lötjönen, "Reconstruction of 3-D Head Geometry From Digitized Point Sets: An Evaluation Study," *IEEE Inf. Technol. Biomed*., vol. 8, pp. 377-386, 2004.

[19] M. Fuchs, J. Kastner, M. Wagner, S. Hawes, and J. Ebersole, "A standardized boundary element method volume conductor model," *Clin. Neurophysiol*., vol. 113, pp. 702-712, 2002.

[20] http://www.mrc-cbu.cam.ac.uk/Imaging/Common/mnispace.shtml#evans_proc

[21] T. F. Oostendorp, J. Delbeke, and D. Stegeman, "The conductivity of the human skull: results of in vivo and in vitro measurements," *IEEE Trans. Biomed. Eng*., vol. 47, pp. 1487-1492, 2000.

[22] http://meshlab.sourceforge.net